polymers, usually with ^2H or ^{13}C. While this method may lead to a direct and unambiguous assignment of the resonance, it can be time consuming and expensive. A simpler, but indirect, approach is to make assignments based on the sequence probabilities and the expected γ-effects on the ^{13}C chemical shifts. The approach is less successful for proton assignments because the spectrum is less resolved and the peaks are insensitive to the γ-effect.

From these studies it is possible to estimate the degree to which 2D NMR may be used to examine more complex systems, which include defects in the polymer chain and several types of monomer units. Most of the 2D spectra reported here required 9–12 h to acquire. At the lowest contour levels we could just see the correlations to the mmm tetrad sequences, which are present to about 8%. 2D NMR of polymer defects less than 1–2% is probably not feasible unless the properties of the defects are considerably different from those of the main chain. The 2D techniques may be successfully applied to more complex polymer systems as long as the resonances from the various monomers are resolved. The use of experiments such as the relayed coherence transfer makes it possible to correlate through longer sections of the polymer chain. In the study of copolymers we expect that this additional information will remove the ambiguities that may complicate the assignment procedure.

References and Notes

(1) Bovey, F. A. "Chain Structure and Conformation of Macromolecules"; Academic Press: New York, 1982.
(2) Bovey, F. A. "High Resolution NMR of Macromolecules"; Academic Press: New York, 1972.
(3) Jeener, J.; Meier, B.; Bachmann, P.; Ernst, R. *J. Chem. Phys.* **1979**, *71*, 4546.
(4) Bax, A. "Two Dimensional Nuclear Magnetic Resonance in Liquids"; Delft University Press: Delft, Holland, 1982.
(5) Wider, G.; Macura, S.; Kumar, A.; Ernst, R. R.; Wüthrich, K. *J. Mag. Reson.* **1984**, *56*, 207.
(6) Macura, S.; Wüthrich, K.; Ernst, R. *J. Mag. Reson.* **1982**, *47*, 351.
(7) Gerig, J. T. *Macromolecules* **1983**, *16*, 1797.
(8) Bruch, M. D.; Bovey, F. A. *Macromolecules* **1984**, *17*, 978.
(9) Gippert, G. P.; Brown, R. L. *Polym. Bull. (Berlin)* **1984**, *11*, 585.
(10) Cheng, H.; Lee, G. *Polym. Bull. (Berlin)* **1984**, *12*, 463.
(11) Bruch, M. D.; Bovey, F. A.; Cais, R. E. *Macromolecules* **1984**, 17, 2547.
(12) Macura, S.; Brown, R. L. *J. Mag. Reson.* **1983**, *53*, 529.
(13) Brown, R. L. *J. Mag. Reson.* **1984**, *57*, 513.
(14) Heatley, F.; Bovey, F. A. *Macromolecules* **1969**, *2*, 618.
(15) Carman, C. J.; Tarpley, A. R.; Goldstein, J. H. *J. Am. Chem. Soc.* **1971**, *93*, 2864.
(16) Maudsley, A.; Müller, L.; Ernst, R. *J. Mag. Reson.* **1977**, *28*, 463.
(17) Bax, A. *Top. Carbon-13 NMR Spectrosc.* **1983**, 197.
(18) Bax, A.; Freeman, R.; Morris, G. *J. Mag. Reson.* **1981**, *42*, 164.
(19) Mareci, T. H.; Freeman, R. *J. Mag. Reson.* **1983**, *51*, 531.
(20) Kessler, H.; Bernd, M.; Kogler, H.; Zarbock, J.; Sorensen, O. W.; Bodenhausen, G.; Ernst, R. R. *J. Am. Chem. Soc.* **1983**, *105*, 6944.
(21) Bolton, P. H. *J. Mag. Reson.* **1982**, *48*, 336.
(22) Wagner, G. *J. Mag. Reson.* **1983**, *55*, 151.
(23) Flory, P. J. "Statistical Mechanics of Chain Molecules"; Wiley Interscience: New York, 1969.
(24) Tonelli, A. E.; Schilling, F. C. *Acc. Chem. Res.* **1981**, *14*, 233.
(25) Bax, A.; Drobny, G. *J. Mag. Reson.* **1985**, *61*, 309.

Effect of Arm Number and Arm Molecular Weight on the Solid-State Morphology of Poly(styrene–isoprene) Star Block Copolymers

David B. Alward,† David J. Kinning, and Edwin L. Thomas*

Department of Polymer Science and Engineering, University of Massachusetts, Amherst, Massachusetts 01003

Lewis J. Fetters

Exxon Research and Engineering Company, Corporate Research Science Laboratories, Clinton Township, Annandale, New Jersey 08801.

Received March 25, 1985

ABSTRACT: The morphological characteristics of star-branched block copolymers having poly(styrene–isoprene) arms (30 wt % polystyrene) have been examined by using electron microscopy, small-angle X-ray scattering, dynamic mechanical thermal analysis, and vapor sorption studies. The special molecular architecture of the star molecules was found to modify the nature of the microphase-separated solid state. The influence of segment molecular weights and star functionality (where f ranged from 2 to 18) on the morphology was examined. In certain cases, e.g., $f \geq 8$, branching brings about the formation of an ordered bicontinuous structure; this structure is not seen in linear materials of equivalent compositions where the equilibrium morphology is that of polystyrene cylinders hexagonally packed in the polydiene matrix.

Introduction

Because of their intrinsic scientific interest and commercial utility, diblock and triblock copolymers have been the subject of intense research since the early 1960s. A clear picture of the morphology of these materials as a function of composition and processing conditions has emerged. However, work on the morphology of star block copolymers is quite limited. This is due to the difficulty of producing well-defined stars in terms of the dispersity of arm number and arm length (molecular weight). The aim of this paper is to examine star block copolymers with the primary emphasis on determining how the special molecular architecture of star molecules modifies the nature of the microphase-separated solid state. The investigative tools are primarily electron microscopy and small-angle X-ray scattering (SAXS), augmented by dynamic mechanical thermal analysis and vapor sorption studies. The polymer samples consist of a series of carefully synthesized poly(styrene–isoprene) star molecules of constant (30 wt % polystyrene) composition with various

*To whom correspondence should be addressed.
†Present address: Monsanto Polymer Products Co., Springfield, MA 01151.

0024-9297/86/2219-0215$01.50/0

arm numbers (2–18) and number-average arm molecular weights (2.3×10^4, 3.3×10^4, and 10×10^4).

Review of Star Block Copolymer Morphology

Before reviewing the microstructure of star block copolymers, the salient morphological features already found for the diblock and triblock systems should be noted. After many years of thorough study[1-5] on the effect of composition and processing conditions on morphology (including selective solvents, casting rate, compression molding, extrusion and annealing times, and temperatures), the picture emerged of a phase-separated domain microstructure in which the minority component always forms the discrete phase and the *equilibrium* morphologies are *ordered arrays* of spheres, cylinders, and lamallae depending on overall composition. With this structural basis firmly established, current work in diblock and triblock systems is now concerned with the details of chain conformation in the various domain geometries, domain interface profiles, order–disorder transitions, agreement with statistical thermodynamic theory, etc.

The number of studies published on the solid-state morphology of star block copolymers is quite small compared to the number of publications on the synthesis of star homopolymers and their behavior in solution and in the melt state as model systems of branched macromolecules. The first study of the effect of arm number on morphology was conducted by Price et al.[6] in 1972 on a series of diblock, triblock, and three- and four-armed block copolymers of isoprene and styrene (using chlorosilane linking agents) keeping the volume percent of the styrene (outer arm) component fixed at approximately 24. Electron microscopy on solvent-cast films showed that hexagonally packed cylindrical domains of polystyrene were formed in a polyisoprene matrix for all arm numbers. In addition, it was reported that arm number had no effect on domain diameter or spacing for two molecular weights.

Bi et al.[7] synthesized and characterized a series of star block copolymers using a divinyl benzene (DVB) linking agent. The polymers, which were not fractionated after synthesis, contained from six to ten arms of a styrene–isoprene diblock, with isoprene at the core of the star, and were composed of approximately 28 vol % polystyrene. The mechanical behavior of the stars was different from the linear block copolymers in four respects; the stars exhibited yielding and had higher strengths, smaller extension ratios, and less permanent set. These features were attributed to the presence of permanent cross-links (the DVB microgel) in the system. The morphological results were different than those obtained by Price et al. on materials of lower arm number and similar but lower PS content. Bi et al. performed electron microscopy on OsO_4 stained sections of solvent-cast, annealed films and determined that the spherical polystyrene domains formed a body-centered array in a polyisoprene matrix. These authors assumed their micrographs depicted a (111) projection of a BCC lattice, while Price et al. were observing "out of plane overlap of the spherical polystyrene domains" which they therfore erroneously assumed to be cylindrical domains of polystyrene.[7]

In a subsequent paper Bi and Fetters[8] investigated the morphology of six- and nine-armed (number average) DVB-linked stars containing ~25 vol % polystyrene. They concluded, on the basis of volume fraction calculations, that the structure consisted of a BCC array of polystyrene spheres in a polyisoprene matrix. However, our reexamination of their original data indicates that the proper interpretation is hexagonally packed cylinders of polystyrene in the polyisoprene matrix, a finding in consonance with that of Price et al.[6]

Expanding on previous work, Bi and Fetters[9] synthesized and studied two series of chlorosilane and DVB linked styrene–butadiene and styrene–isoprene star block copolymers containing from 3 to 29 branches and approximately 27 to 40 vol % polystyrene (outer block). Although the main thrusts of this paper were synthesis, characterization, mechanical properties, and dynamic mechanical properties, the structure for the majority of the samples was briefly discussed, incorrectly, as being a BCC array of spheres of PS in a rubbery matrix. Although not specifically stated, one might assume, therefore, that there is no effect of arm number or molecular weight on equilibrium domain structure at these compositions as well. In addition, the authors mentioned that there was no effect of solvent type on the morphology of cast films and almost no change in structure when the films are annealed.

Pedemonte et al.[10] published a paper on the mechanical properties and morphology of some four-armed stars produced by the Anic Co. and known as Europrene T-162. This is a tetrachlorosilane-linked star consisting of approximately 50% each of polystyrene and polybutadiene, with polybutadiene at the core. The performance of microtomy and microscopy on compression-molded films in three directions showed the structure consisted of short rods of polystyrene that were aligned perpendicular to the plane of compression. From our examination of their micrographs, there appears to be very little difference in the appearance of the films cut in the different directions; the structure appears to correspond closely to almost any block copolymer system of similar composition formed under highly nonequilibrium conditions. Additional proof of the anisotropic nature of the film would have been desirable. Nevertheless, the authors are able to rationalize various aspects of the mechanical behavior, such as necking and strain softening, in terms of this model of short rods of polystyrene oriented perpendicular to the compression plane.

Meyer and Widmaier[11] studied the adhesion behavior of 2–13-armed stars consisting of DVB, silicon tetrachloride, and tetrakis(chloromethyl 1,2,4,5)benzene linked arms of styrene–isoprene diblocks and styrene–isoprene–styrene triblocks. The stars with diblock arms consisted of approximately 50% polystyrene, and the stars with triblock arms contained 70% polystyrene. No morphological studies were made, but it was found that the stars were better adhesives than the corresponding linear molecules. The difference was attributed to the relatively high cohesive strength of the stars due to the introduction of physical cross-links and the formation of a large, central, glass domain consisting of DVB plus polystyrene.

A quite thorough paper by LeBlanc on the processing-property relationships of some four-armed stars appeared in 1977.[12] The materials studied were styrene–butadiene Solprene resins supplied by the Phillips Petroleum Co., which were compared to the more conventional linear triblock Kraton resins manufactured by the Shell Co. The important conclusions concerning the mechanical behavioral differences between the linear triblock and four-armed star are that the star samples show a higher Youngs' modulus, a greater tendency to exhibit yielding, and a greater dependence of molecular weight on modulus, yield stress and strain, and ultimate stress and strain. No observations on the sample morphologies were reported.

In summary, the study of the solid-state behavior and morphology of star block copolymers is much less advanced than the corresponding study of linear block copolymers. The published works that have been discussed do not

Table I
Poly(styrene-isoprene) Star Block Copolymer Samples

arm mol wt		
polystyrene	total × 10^{-4}	no. of arms
7×10^3	2.3	2, 4, 8, 12, 18
1×10^4	3.3	2, 4, 8, 12, 18
3×10^4	10	4, 12, 18

present a conclusive picture of the solid-state structure of these materials. There are disagreements in the results and really very little systematic work on the effect of arm number and arm molecular weight on microstructure. It was from this standpoint that the work presented in this paper was undertaken.

Experimental Methods

Sample Synthesis and Characterization. The chlorosilane method was used to prepare the star block copolymers. For more detail, the reader is referred to the original work[13,14]. The nomenclature used to describe the samples is as follows: 18/30/10 is an 18-armed star containing 30 (±1) wt % polystyrene, the molecular weight of the polystyrene block in each arm being 1.0×10^4. Stars of 2 (i.e., a linear triblock), 4, 8, 12, and 18 arms were synthesized. All were composed of 30 wt % (approximately 27 vol %) polystyrene with the polyisoprene block at the core of the star. Arm molecular weights of 2.3×10^4, 3.3×10^4, and 10×10^4 were prepared (see Table I).

The purifications of the monomers and solvents were performed under high vacuum, as were the polymerizations. *sec*-Butyllithium was the initiator used, and benzene was the solvent. Polymerizations to form the arms were performed at 30 °C, while the reaction of the multifunctional linking agent with an excess of active centers was carried out at 40 °C for a period of several days to a week. The reactions were terminated with degassed methanol. Careful fractionation of the reaction product readily separated the unreacted diblock from the branched star material.

Number-average and weight-average molecular weights for the linear arm precursors and star molecules were determined by high-speed membrane osmometry or by light scattering (the latter for the higher molecular weight samples). This enabled an estimation of the functionality of the star to be made. Gel permeation chromatography was used to evaluate the molecular weight polydispersity. The microstructure of the polyisoprene block in the chain was studied by ^{1}H NMR spectroscopy and determined to contain ca. 70% cis 1,4 linkages, 24% trans 1,4 linkages, and 6% 3,4 linkages. Polydispersities of 1.05 or less were typical of the linear arm precursor, while functionalities of approximately 3.9, 7.8, 11.7, and 17.6 were achieved for the 4-, 8-, 12-, and 18-armed stars, respectively. These functionalities are in agreement with the characterization results available elsewhere[13-16] for multiarmed star polymers prepared by use of the appropriate chlorosilane linking agents. Examples of size exclusion chromatograph (SEC) traces for a polystyrene segment of a diblock arm, a diblock arm, an unfractionated eight-armed star, and the fractionated eight-armed star (8/30/10) are shown in Figure 1.

Sample Preparation. Since our interest is in the solid-state order of these materials, sample preparation conditions were employed to promote the system to achieve thermodynamic equilibrium (i.e., avoid preferential solvents, quick casting, or thermoforming techniques). The as-prepared samples containing a small amount of antioxidant (<0.25%) were dissolved in a nonpreferential solvent, toluene, to make 3% w/v solutions. A volume of solution required to produce polymer films 1.0–1.5 mm thick was placed in a covered beaker in an oven (45 °C) at atmospheric pressure. Approximately 1 week was required under these conditions for solvent evaporation. Next, individual samples were placed in small tubes and connected to a high (10^{-5} torr) vacuum line. After 12 h of pumping, the tubes were sealed off with a torch. The sealed tubes were then placed in a vacuum oven for 2 weeks at temperatures of 95, 110, and 125 °C for the low, medium, and high arm molecular weight series, respectively. These annealing temperatures were chosen to be above the T_g of the polystyrene component and below the order-to-disorder transition temperature (ca. 145 °C[17] in high molecular weight polystyrene–polyisoprene systems). From the morphologies observed, it was evident that the annealing treatments were not equally successful. The two series having the lower molecular weight arms displayed good order and a small amount of viscous flow during annealing. The series with the highest arm molecular weight developed order not greatly improved over that of the as-cast films. These films also retained their original shape during the annealing treatment as a consequence of their high molecular weight.

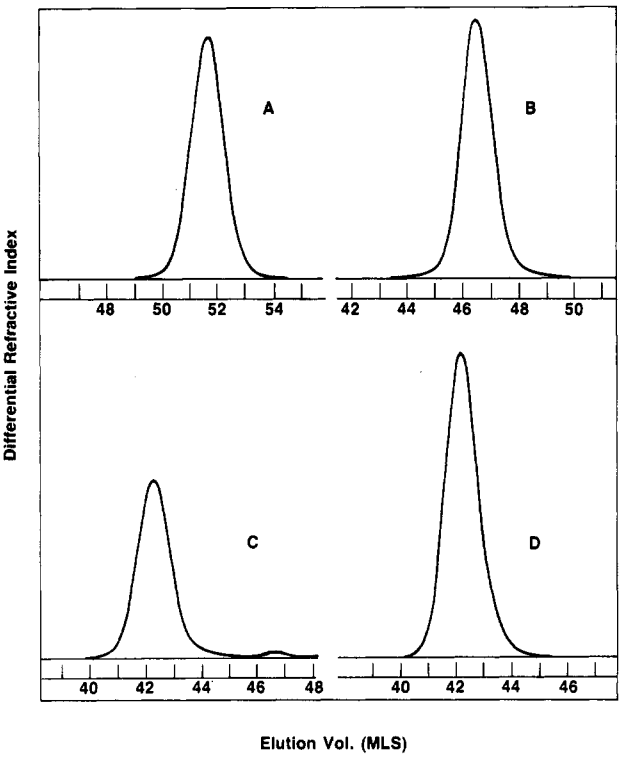

Figure 1. Size exclusion chromatographs of (a) polystyrene segment of diblock arm, (b) poly(styrene–isoprene) diblock arm of 8/30/10 star block copolymer, (c) unfractionated 8/30/10 star block copolymer, and (d) fractionated 8/30/10 star block copolymer.

Cryoultramicrotomy and Staining and Electron Microscopy. An AO Reichert Ultracut microtome with FC4 cryo attachment was used with a diamond knife to produce thin sections. Sample and knife temperatures of −95 °C were employed with isopropyl alcohol for floating sections. Sections were picked up on 700-mesh copper grids and then placed in the vapors of a 4% osmium tetroxide–water solution for 4 h for selective staining of the polyisoprene phase.

A JEOL 100CX Temscan electron microscope operated at 100 kV was used to examine the samples. The side-entry goniometer and single-tilt holder allowed tilts of up to ±60°, enabling single grains of the domain microstructure to be imaged over a wide range of tilting angles. Bright-field imaging was done by using a 10 Å^{-1} objective aperture, and the micrographs were recorded on Kodak SO-163 image plates.

Small-Angle X-ray Scattering. Small-angle X-ray scattering was performed by using a 1-kW nickel-filtered copper source and Kratky collimation. The collimation block and flight path were evacuated, but there was a 10-cm air path in the region of the sample holder. The camera was aligned with a 40-μm entrance slit and a 12-mm beam limiter. Scattered radiation was collected with a Braun one-dimensional position-sensitive detector operated at 11-bar pressure of 90% argon–10% methane gas and 3.8 kV, for which the spatial resolution is better than 50 μm. The sample-to-detector distance of 50 cm yielded an angular (2θ) resolution of approximately 0.2 mrad. The scattering data were corrected for sample absorption, wire sensitivity, and parasitic scattering. Slit-length desmearing was done by using Vonk's FFSAX Version 3 program.[18]

Dynamic Mechanical Analysis. A dynamic mechanical thermal analyzer (Polymer Labs) was used to generate curves of the log of the Young's modulus (log E') vs. temperature. Sample

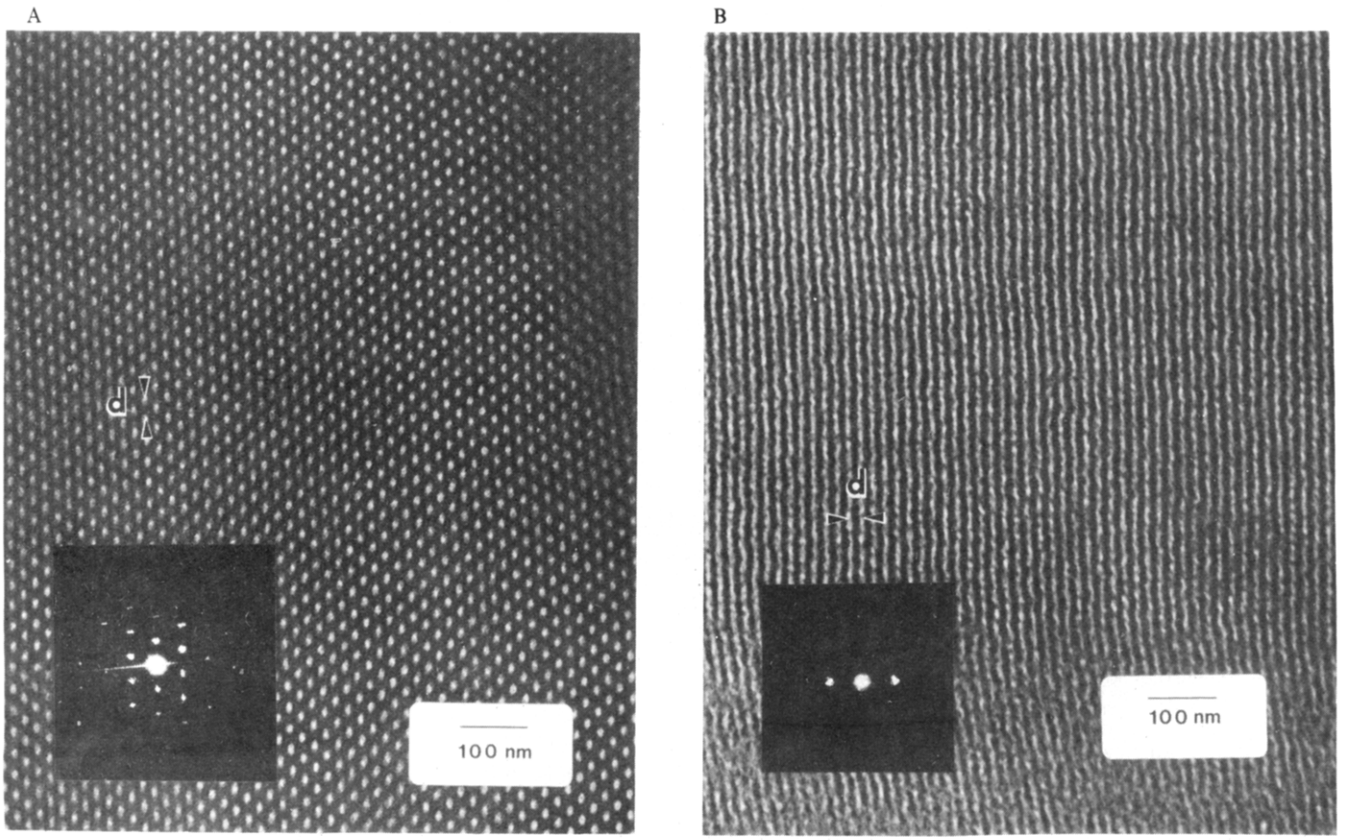

Figure 2. Cylindrical morphology of sample 4/30/10: (a) axial view (and its optical transform (inset)) showing the intercylinder spacing; (b) longitudinal view of cylinders.

dimensions were approximately 10 mm × 5 mm × 1 mm, as required for clamping, while the actual volume of material tested was on the order of 1 mm (L) × 5 mm (H) × 1 mm (T). The machine was used in the single-cantilever mode (due to the limited amounts of some samples) at a strain rate of 1 Hz and a scan rate of 5 °C min^{-1}. The data showed evidence of sample clamping problems as the glass-transition temperature of the polystyrene was approached, but data in the −90 to +70 °C range were reproducible. A further problem encountered was the relatively inaccurate nature of the temperature read-out of the Polymer Labs' instrument. Nonetheless, the results obtained from this instrument exhibited reproducible precision, thus rendering the relative comparison of the various samples meaningful.

Sorption Measurements. The apparatus used for sorption measurements consisted of a gas delivery system and a Cahn Model 2000 quartz spring electrobalance. The mass of the sample was monitored continuously within ±2 μg with the output to a chart recorder. The sample dimensions were approximately 2 cm × 2 cm × 0.1 cm, so that the diffusion equation could be solved for the one-dimensional slab geometry case and a value of the effective diffusion coefficient of the penetrant gas calculated. Sorption experiments were performed at room temperature. Three different penetrant gases (CO_2, O_2, and N_2) were used.

Results and Discussion

Microstructure by Electron Microscopy. Transmission electron microscopy is one of the most useful techniques for the characterization of ordered block copolymer morphologies in the solid state. For proper analysis of micrographs from ordered lattices, it is essential that the microscopist bear in mind that the image seen represents a two-dimensional projection of the three-dimensional structure. This is a disadvantage in the study of systems in which small domains are randomly distributed in a matrix phase. Although there could be a phase-separated structure in the film, the microscopist would not be able to distinguish the micrograph of this randomly arranged phase-separated structure from a micrograph containing only random noise effects.[19] This is for two reasons: (1) the domain dimensions are small compared to the thickness of the film and (2) the lack of order in the sample precludes the occurrence of constructive overlap of domains.

Relatively thick (~1000 Å) sections are usable for ordered block copolymer systems because domains will project onto one another for certain orientations. For example, the two easily interpretable projections of hexagonally packed cylinders are the axial projection (a hexagonal array of circular domains) and the longitudinal projection (a series of alternating stripes).

At 30 wt % polystyrene, that is, ~27 vol % polystyrene, diblock and triblock copolymers form (see Molau's representation[20]) an equilibrium morphology of polystyrene cylinders hexagonally packed in a matrix of polyisoprene. This morphology is observed in our star block copolymers of low arm number and/or molecular weight. Figure 2a shows a micrograph and optical transform of an axial projection of this structure for the 4/30/10 sample. Figure 2b shows the longitudinal projection of cylinders and its corresponding optical transform. Both projections must be present in the film to distinguish the morphology from hexagonally packed spheres or parallel lamellae viewed edge on. This cylindrical (CYL) morphology is found for all the triblock and 4-armed samples as well as for the 8- and 12-armed samples of the 7000 molecular weight series (see Table II).

The higher arm number and molecular weight samples exhibit a strikingly different morphology (see Figure 3). The 18-armed samples in the 2.3×10^4 molecular weight series, the 8-, 12-, and 18-armed samples in the 3.3×10^4 molecular weight series, and the 12- and 18-armed samples in the 1.0×10^5 molecular weight series form what we shall hereinafter refer to as the ordered bicontinuous (OB) morphology. Specific details of this OB structure will be

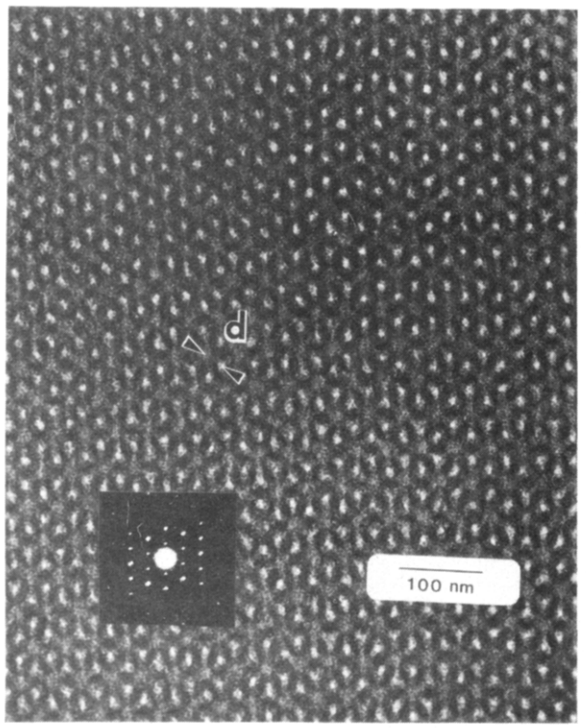

Figure 3. High-contrast, high-symmetry view of the ordered bicontinuous structure. This wagon-wheel arrangement is identical with that given previously, without discussion, by Aggarwal[42] for the star block copolymer $(SI)_{15}$-DVB-12 of ref 9, containing 30 wt % polystyrene.

presented in a future paper.[21] It is a structure decidedly different from the normal sphere, cylinder, and lamella structures of diblocks and triblocks. Hence the molecular architecture of the star molecules can induce a new equilibrium solid-state microstructure at constant composition either through an increase in the number of arms of the star or by an increase in the arm molecular weight.

Table II
Structural Parameters of Star Block Copolymer Samples

arm molecular weight	EM	arm no. 2	4	8	12	18
2.3×10^4		CYL	CYL	CYL	CYL	OB
	d_1, EM	200	205	225	180	220
	d_1, SAXS	246	224	228	197	250
	d_2/d_1	0.58	0.57	0.58		
	d_3/d_1	0.51		0.50		
	d_4/d_1					
3.3×10^4		CYL	CYL	OB	OB	OB
	d_1, EM	220	225	220	220	215
	d_1, SAXS	268	270	242	245	250
	d_2/d_1	0.60	0.59	0.86	0.85	0.83
	d_3/d_1		0.49	0.75	0.74	0.74
	d_4/d_1			0.57	0.58	0.58
1.0×10^5			CYL		OB[a]	OB[a]
	d_1, EM		330			
	d_1, SAXS		417		423	444
	d_2/d_1		0.50		0.73	0.56
	d_3/d_1				0.58	
	d_4/d_1					

[a] Samples are rather poorly ordered.

Before proceeding to other techniques to help in the detailed analysis of the OB structure, it should be mentioned that Figure 3 is only one particular high-symmetry, high-contrast projection of the OB structure. Unlike the cylindrical structure, which exhibits in a typical section a significant area of nearly uniform gray contrast due to lack of positive overlap of domains in the projection (see Figure 4a), the ordered bicontinuous structure exhibits many high-contrast grains (see Figure 4b). Assuming that the grains in both samples possess nominally random relative orientations with respect to the section surface, one may deduce that the OB structure has higher struc-

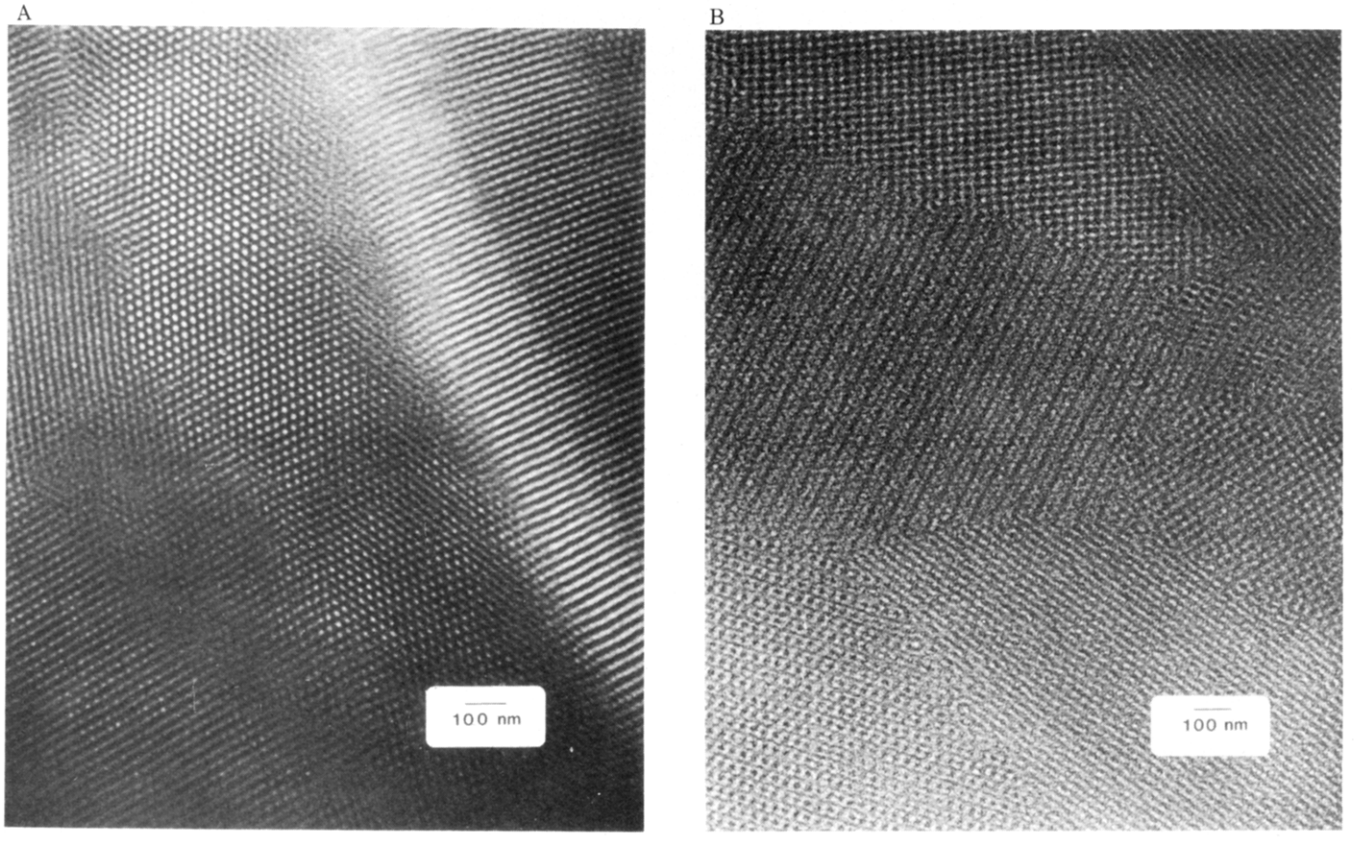

Figure 4. "Typical" views of (a) cylindrical morphology and (b) ordered bicontinuous morphology.

tural symmetry than the cylindrical structure. That is, if one views the structure along a random direction, it is more likely a high-contrast projection will be seen in the OB structure. That these high-contrast projections all belong to just a single OB structure is demonstrated via tilt experiments where one projection is converted into another (e.g., see Figure 5a,b).

Small-Angle X-ray Scattering Studies. The scattering behavior from these materials falls into three categories. The first set of samples is exemplified by a single interference peak. Because SAXS is sensitive to global order and block copolymer lattices are highly paracrystalline, one can conclude from the absence of higher order peaks that the lattice perfection is not highly developed in these samples. Even when selected areas appear relatively well-ordered by electron microscopy, SAXS results, which depend on the average over a large volume, can indicate an overall lack of order.

The second set of samples exhibits a higher order interference peak corresponding to a spacing of approximately 0.58 that of the first peak spacing (d_1). Some possible d_2/d_1 ratios are 0.707 for the simple cubic (SC) and body-centered cubic (BCC) lattices, 0.866 for face-centered cubic (FCC) lattices, 0.612 for diamond cubic (DC) lattices, and 0.577 for hexagonally packed cylinders. Comparison of the d_2/d_1 ratios to the electron microscopy results shows conformation of the cylindrical morphology in each case. An example of the SAXS pattern from a cylindrical sample (4/30/10) is given in Figure 6a. The position of the broad peak at higher angle (arrowed) relates to the form-factor scattering from the cylinders. The calculated cylinder diameter based on the form-factor peak is 150 Å, in reasonable agreement (considering the known effect of OsO_4 staining to cause dimensional changes[22]) with the electron microscopy results (100 Å) for this sample (see Figure 2).

The third set of samples shows three higher order peaks at d_n/d_1 ratios of approximately 0.84, 0.74, and 0.57. These ratios do not correspond to any of the five simple structures discussed previously. Figure 6b shows a SAXS pattern from this type of sample (18/30/10).

In summary, the SAXS results showed the same cylinder-to-ordered bicontinuous transition with arm number and with arm molecular weight as the electron microscopy results. That is, all samples shown by SAXS to exhibit a higher order peak at approximately 0.6 d_1 were shown by electron microscopy to be cylindrical, and all SAXS patterns displaying higher order peaks at approximately 0.84, 0.74, and 0.57 d_1 were shown by electron microscopy to possess the ordered bicontinuous morphology. Also, SAXS indicates that the OB structure is clearly different from the structure consisting of a hexagonal array of parallel cylinders, although possible assignments of the OB structure based on its relatively complex SAXS pattern remain to be proposed.[21]

Dynamic Mechanical Thermal Analysis. Dynamic mechanical thermal analysis (DMTA) measures the in-phase and out-of-phase moduli of a material as a function of temperature. If the material tested has phases of widely varying glass-transition temperatures, DMTA can provide information about phase mixing and distribution of phases within the material. In general, systems containing discrete glassy domains in a rubbery matrix will exhibit room-temperature moduli characteristic of a vulcanized rubber (ca. 1–5 MPa) because of the reinforcing action of the polystyrene domains. Systems in which a glassy matrix phase contains discrete rubber domains will have room-temperature moduli ca. 1 GPa, close to those of the pure glassy component. As a guide to the magnitude of the expected change in room-temperature modulus of a glassy continuous vs. rubbery continuous material, the upper and lower bounds of the composite modulus may be calculated by the Kerner equation,[23-25] which assumes dispersed spherical domains of the discrete phase. At 30 vol % polystyrene the glassy continuous composite modulus is about 400 times greater than the rubbery continuous composite modulus.

Various workers[26-28] have noted the effect of enhanced polystyrene continuity on dynamic mechanical and tensile behavior of styrene–isoprene–styrene triblock copolymers induced by employing a polystyrene preferential solvent. This is manifested in a less severe decrease in storage modulus when temperatures are scanned up through the glass transition of the polyisoprene phase and in a distinct yield point and visible neck in tensile tests.

The $E'(T)$ curves (e.g., see Figure 7) of the star block copolymers show a glassy plateau in log E' at temperatures below the glass-transition temperature of both components. As the temperature is increased, the glass transition of the polyisoprene is reached and the material exhibits a sharp drop in the storage modulus. Another plateau region then persists until the glass-transition temperature of the polystyrene phase is reached. At this point, acquisition of reliable data using this apparatus becomes difficult because the sample can no longer be securely gripped.

The log $E'(T)$ curves for the cylindrical samples all display behavior in good agreement with that of SIS and SBS triblocks of similar composition and morphology presented in the literature. In particular, the drop of $E'(T)$ is by about a factor of 100 over the range of −90 °C to room temperature. The behavior of all the OB samples departs from this norm, showing a drop in modulus of only a factor of 10 over the same range. The discontinuous transition in mechanical behavior as arm molecular weight is increased is also seen in the plots of tan δ vs. temperature (Figure 8). Thus we have a very consistent mechanical picture of the transition from the CYL to OB structure with the further important fact that there is a significantly enhanced continuity of the polystyrene phase in the OB samples.

Sorption Experiments. Initially, pure polystyrene and pure polyisoprene were examined to see if Fickian behavior was obeyed for diffusion of simple gases. This behavior was indeed observed, as sorption and desorption curves were superposable for O_2, N_2, and CO_2 gases. The effective diffusion coefficient, D_{eff}, was calculated from the half-time method, the initial slope method, as well as the moment method. All three methods give consistent results for all three gases in both the pure components and block copolymer systems. A detailed discussion of sorption measurements in multiphase polymers is given in ref 29. Since the diffusion of gases in polyisoprene is about 40 times faster than in polystyrene, the measurement of D_{eff} should allow an unambiguous determination of whether polyisoprene phase continuity exists.

The sorption results quite clearly and consistently show for all combinations of permeant and calculation methods that the effective diffusion coefficients for the various star block copolymer samples indicate a polyisoprene continuous structure. For example, the value of the effective diffusion coefficient for the 4/30/10 sample (cylindrical), which is known to be polyisoprene continuous, is virtually identical to the value for the 18/30/10 sample (OB) (see Table III). That the polyisoprene phase is continuous in the OB morphology is another important fact about this structure.

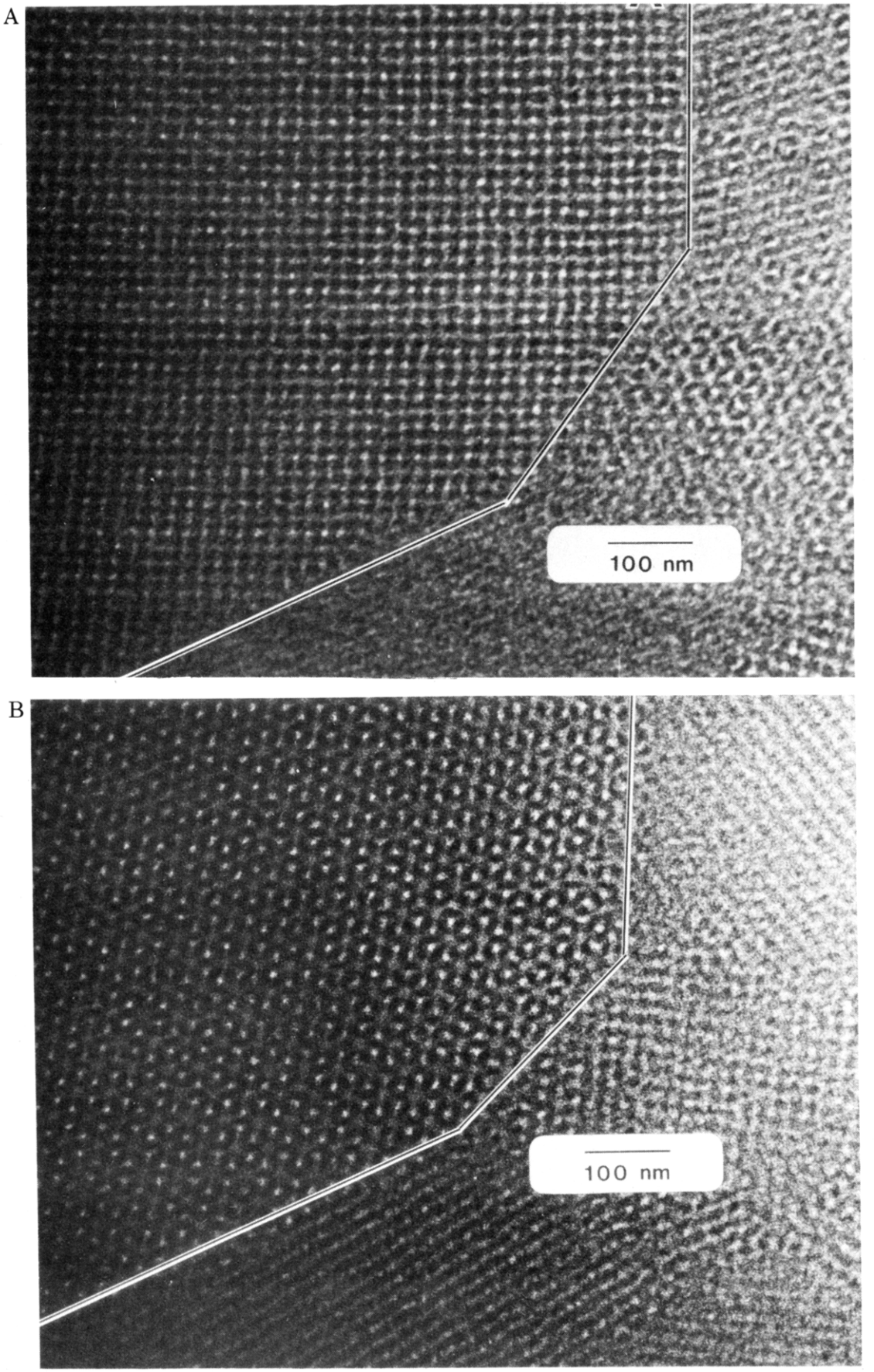

Figure 5. Pair of micrographs illustrating how a grain of the OB structure converts from the square projection (a) into the wagon-wheel projection (b) by appropriate tilt of the specimen.

Effect of Arm Number on Interdomain Distance for Identical Structures. There are three groups of samples to examine, neglecting the 1.0×10^5 molecular weight series because of their lack of well-developed order. The groups to consider are the 2/30/7, 4/30/7, 8/30/7, and 12/30/7 (cylindrical), the 2/30/10 and 4/30/10

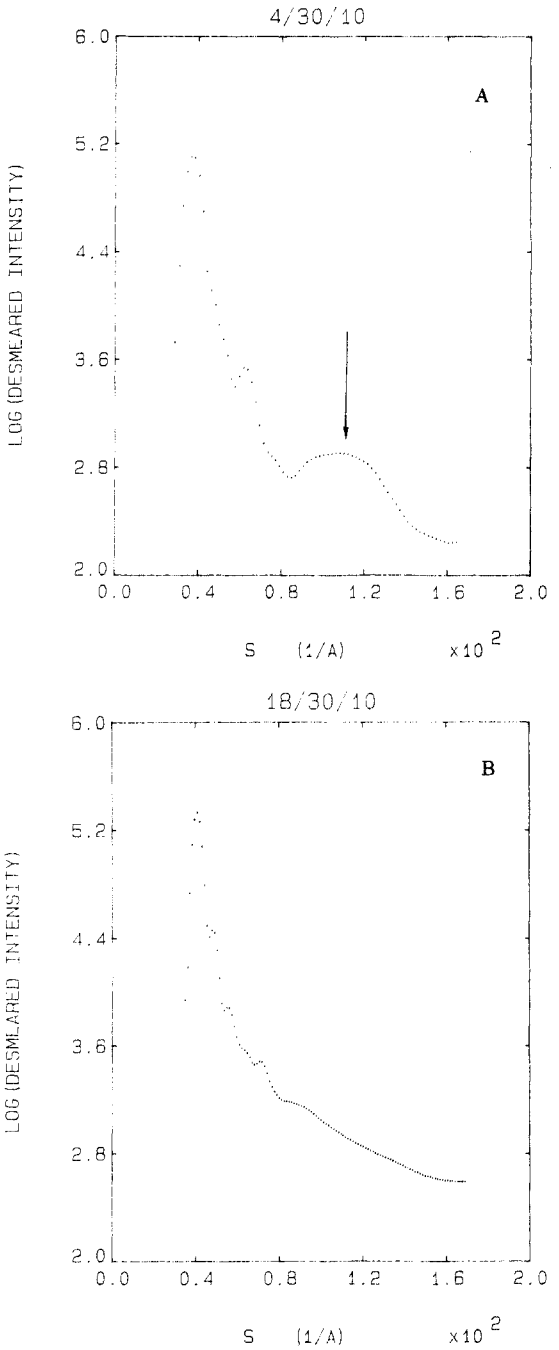

Figure 6. Small-angle X-ray scattering patterns of (a) sample 4/30/10 (cylindrical morphology) and (b) sample 18/30/10 (ordered bicontinuous morphology).

Table III
Sorption Data: Effective Diffusion Coefficient of O_2 at 22 °C

	initial slope	half-time	limiting slope
PS	1.2×10^{-7}	1.2×10^{-7}	1.3×10^{-7}
PI	4.5×10^{-6}	4.6×10^{-6}	4.3×10^{-6}
4/30/10 (CYL)	7.9×10^{-7}	1.0×10^{-6}	1.3×10^{-6}
18/30/10 (OB)	6.4×10^{-7}	8.9×10^{-7}	1.4×10^{-6}

(cylindrical), and the 8/30/10, 12/30/10, and 18/30/10 (OB). Taken in turn, the first group possess an average (EM and SAXS) spacing slightly larger than that predicted (180 Å) for cylindrical domains of 7.0×10^3 molecular weight styrene by using the Helfand and Wasserman calculation[30] with no trend with increasing arm number. Similarly there is no effect of arm number on the intercylinder spacing for the 2/30/10 and 4/30/10 samples. The calculated value of an interdomain spacing of 220 Å

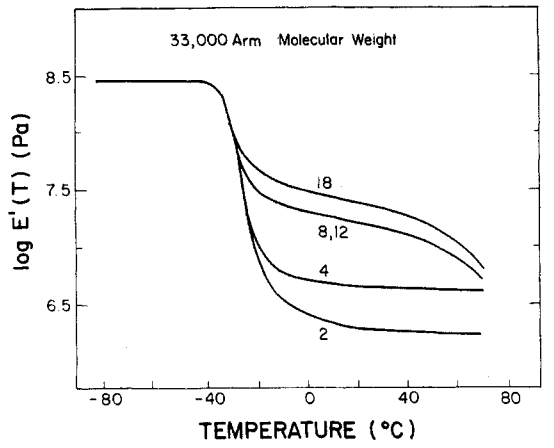

Figure 7. Dynamic mechanical storage modulus as a function of temperature for a series of 2–18-armed star block copolymers, all with 3.3×10^4 arm molecular weight.

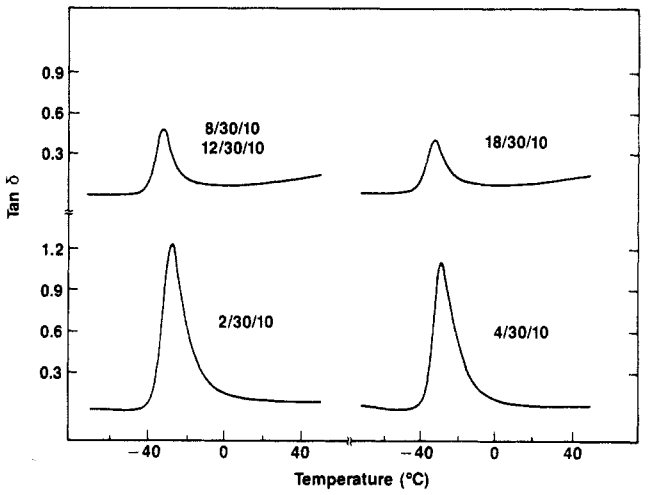

Figure 8. Dynamic mechanical loss tangent as a function of temperature for a series of 2–18-armed star block copolymers, all with 3.3×10^4 arm molecular weight.

for the 1.0×10^4 molecular weight polystyrene is again smaller than that measured experimentally. These results on the cylindrical samples are in accord with those of Price et al.,[6] who found no difference in intercylinder spacing in the two-, three-, and four-armed star block copolymers he examined. Finally, for the OB structure of the 3.3×10^4 molecular weight series, the interdomain distance does not change as the arm number increases from 8 to 12 to 18. Indeed, the interdomain spacing for the entire series of arm numbers for a given molecular weight remains approximately constant regardless of the particular morphology.

Effect of Molecular Weight on Interdomain Distance for Identical Structures. From Table II one sees that for a constant arm number of four, increasing arm molecular weight, as expected, increases the interdomain distance for the cylindrical samples. The same is true for the three 18-arm OB samples. With the limited number of samples and range of molecular weights explored, it is not possible to derive a precise molecular weight power law dependence for the interdomain spacing for each of the structures.

Cylinder-to-OB Transition. The expected morphology for diblock and triblock copolymers for the composition studied (30 wt % polystyrene) is hexagonally packed cylinders. The molecular architecture of star molecules is seen to affect the equilibrium phase-separated morphology at this particular overall composition only at high

arm number and high arm molecular weight. There is a transition from the cylinder to the OB structure between 12 and 18 arms for the 2.3×10^4 molecular weight series, between 4 and 8 arms for the 3.3×10^4 molecular weight series, and between 4 and 12 arms for the 1.0×10^5 molecular weight series.

First we address the influence of arm number. This effect can be loosely rationalized in terms of excluded volume. As more and more arms are added to the central linking agent, overcrowding of polyisoprene segments at the core of the star forces the core region to assume a more spherical shape. That is, the molecular trajectories of the arms will tend to be radial, especially near the core of the star where the overcrowding is most severe. This overcrowding has been theoretically predicted[31-40] and observed experimentally.[15,16] The free end of the arm, however, contains polystyrene, and therefore the junction point (isoprene–styrene bond) of the arm must be placed at the domain boundary. In effect, this presents an energy minimization problem with two separate facets: (1) conformational restriction of junction placement, maintenance of constant density, and the surface area to volume ratio considerations (the usual situation for diblock and triblock copolymers) and (2) the limitations imposed on the system by the conformational restriction for the inner block. It can then be argued that favorable microstructures particular to star block copolymers are those in which the domain structure is arrayed such that the arms can take approximately radial trajectories toward the domain boundary from the star center. When the second term makes a relatively small contribution to the overall free energy of the system or when its contribution is such to promote a particular linear block phase-separated microstructure, the phase-separated state of the star block copolymer will follow that expected for the linear block copolymer of that particular composition. However, when the second term makes a significant contribution to the overall free energy but calls for a *different* microstructure, a compromise must be struck and the phase-separated state of the star block copolymer may exhibit new structures.

The situation is asymmetrical with respect to overall composition due to the unique constraint on the *inner* block units of the star copolymer. For low volume fractions of the inner block, the favored geometry would be spherical domains of the inner block component (i.e., no change in structure from the linear block case). As the volume fraction of inner block increases, a transition to cylindrical geometry would be expected, perhaps at a somewhat higher volume fraction than the linear case. In the mid-range of compositions, the system would likely be lamellar. At still higher inner block volume fraction (such as the present 73% volume fraction polyisoprene samples), the normal inverted cylindrical and inverted spherical morphologies present adverse situations, since it is now the lower volume fraction outer block chains that reside on the negative curvature side of the domain interface. Thus, depending on the relative magnitude of the second term, new structural states may be found in the high inner block compositional range. The dependence of star block copolymer morphology on overall composition at constant arm number is the subject of another paper.[41]

In the present case of 73 vol % inner block, the interconnected bicontinuous structure may represent such a compromise structure. A possible kinetic pathway to the linked network is the clustering and compaction of close-packed spherical micelles with polyisoprene centers and outer spherical shells of polystyrene upon solvent evaporation into a polyisoprene matrix containing a continuous polystyrene framework.

The preceding argument for the appearance of the novel OB microstructure is based on the increased overcrowding at the core of the star resulting in the transition from cylindrical geometry to a more favorable phase-separated microstructure. This line of reasoning, however, leads to quite the *opposite* prediction of the effect of arm molecular weight on the transition at constant arm number, since as the molecular weight increases, the fraction of the chain experiencing overcrowding decreases. In the limit of infinite chain length, the polyisoprene–polystyrene junction point should not be influenced by the core of the star, and the problem should revert to the situation for phase separation of linear block copolymers. This discrepancy points toward the probable omission of an important factor in the free energy balance.

Summary and Conclusions

The goal of this research was an elucidation of the influence of molecular topology on the development of equilibrium phase-separated morphologies in multiarmed block copolymer systems. Transport measurements, dynamic mechanical thermal analysis, small-angle X-ray scattering, and electron microscopy were used to directly and indirectly probe the morphologies.

The samples studied were of constant composition (30 wt % polystyrene at the free end of the arm). The stars examined had 2, 4, 8, 12, or 18 arms and total arm molecular weights of 2.3×10^4, 3.3×10^4, and 10×10^4.

It was shown that a transition from the cylindrical morphology of hexagonally arrayed polystyrene domains in a polyisoprene matrix to a new ordered bicontinuous morphology occurred, dependent on both the number of arms per star and the molecular weight of the arm. As the number of arms increases or the molecular weight of the arm increases, the ordered bicontinuous morphology is thermodynamically favored. Thus, although all the star block copolymers examined contain 27 vol % polystyrene and would form a polystyrene cylindrical microstructure were it not for the influence of star core at high arm number and high arm molecular weight, they prefer a morphology such that the polystyrene end block is accommodated in a polystyrene domain in a more three-dimensionally symmetric nature. This is allowed by the ordered bicontinuous structure.

The effect of arm molecular weight on the cylindrical to ordered bicontinuous transition is at present not understood. Extending the overcrowding argument, we would expect the core region of the star to have less influence on the position of the junction point between respective blocks as the fraction of the material in the core region decreases (arm molecular weight increases). This should enable the A–B interaction/junction placement/density maintenance/surface area–volume features of diblocks and triblocks to rule the structure, forming cylinders. However, the opposite effect of arm molecular weight is found.

Acknowledgment. The financial support of the Polymer Division, NSF, through Grants DMR80-12724 and DMR84-06079 and the Monsanto Corp. for a fellowship for D.B.A. is greatly appreciated. We thank Dr. D. L. Handlin, Jr., for useful discussions and Dr. J. E. Sax for making the vapor sorption measurements.

References and Notes

(1) Aggarwal, S. L., Ed. "Block Polymers"; Plenum Press: New York, 1970.
(2) Molau, G. E., Ed. "Colloidal and Morphological Behavior of Block and Graft Copolymers"; Plenum Press: New York, 1971.

(3) Folkes, M. J.; Keller, A. In "Physics of Glassy Polymers"; Harwood, R. N., Ed.; Applied Science: London, 1973; p 548.
(4) Gallot, B. R. M. *Adv. Polym. Sci.* **1978**, *29*, 85.
(5) Goodman, I., Ed. "Developments in Block Copolymers"; Applied Science: New York, 1982; Vol. I.
(6) Price, C.; Watson, A. G.; Chow, M. T. *Polymer* **1972**, *13*, 333.
(7) Bi, L. K.; Fetters, L. J.; Morton, M. *Polym. Prepr. (Am. Chem. Soc., Div. Polym. Chem.)* **1974**, *15*(2), 157
(8) Bi, L. K.; Fetters, L. J. *Macromolecules* **1975**, *8*, 90.
(9) Bi, L. K.; Fetters, L. J. *Macromolecules* **1976**, *9*, 732.
(10) Pedemonte, E.; Dondero, G.; deCandia, F.; Romano, G. *Polymer* **1976**, *17*, 72.
(11) Meyer, G. C.; Widmaier, J. M. *Polym. Eng. Sci.* **1977**, *17*(*11*), 803.
(12) LeBlanc, J. L. *J. Appl. Polym. Sci.* **1977**, *21*, 2419.
(13) Hadjichristidis, N.; Guyot, A.; Fetters, L. J. *Macromolecules* **1978**, *11*, 668.
(14) Hadjichristidis, N.; Fetters, L. J. *Macromolecules* **1980**, *13*, 191.
(15) Roovers, J.; Hadjichristidis, N.; Fetters, L. J. *Macromolecules* **1983**, *16*, 214.
(16) Huber, K.; Burchard, W.; Fetters, L. J. *Macromolecules* **1984**, *17*, 541.
(17) Chung, C. I.; Griesbach, H. C.; Young, L. *J. Polym. Sci., Polym. Phys. Ed.* **1980**, *18*, 1237, 1242.
(18) Vonk, C. *J. Appl. Crystallogr.* **1975**, *8*, 340.
(19) Roche, E. J.; Thomas, E. L. *Polymer* **1981**, *22*, 333.
(20) Molau, G. E. In "Block Copolymers"; Aggarwal, S. L., Ed.; Plenum Press: New York, 1970; p 76.
(21) Kinning, D. J.; Alward, D. B.; Thomas, E. L.; Fetters, L. J., in preparation.
(22) Berney, C. V.; Cohen, R. E.; Bates, F. S. *Polymer* **1982**, *23*, 1222.
(23) Kerner, E. H. *Proc. Phys. Soc., London* **1956**, *B69*, 802.
(24) Dickie, R. A. In "Polymer Blends"; Paul, D. R.; Newman, S., Eds.; Academic Press: New York, 1978; Vol. I, p 353.
(25) Nielsen, L. E. *Rheol. Acta* **1974**, *13*, 86.
(26) Beecher, J. F.; Marker, L.; Bradford, R. D.; Aggarwal, S. L. *J. Polym. Sci., Part C* **1969**, *26*, 117.
(27) Shen, M.; Cirlin, E. H.; Kaelble, D. H. In "Colloidal and Morphological Behavior of Block and Graft Copolymers"; Molau, G. E., Ed.; Plenum Press: New York, 1971; p 307.
(28) Kotaka, T.; Miki, T.; Arai, K. *J. Macromol. Sci., Phys.* **1980**, *B17*, 303.
(29) Felder, R. M.; Huvard, G. S.; "Permeation, Diffusion and Sorption of Gases and Vapors", in "Methods of Experimental Physics"; Fara, R., Ed.; Academic Press: New York, 1980; Vol. 16C.
(30) Helfand, E.; Wassermann, Z. R. In "Development in Block Copolymers"; Goodman, I., Ed.; Applied Science: New York, 1982; Vol. I, p 99.
(31) Daoud, M.; Cotton, J. P. *J. Physique* **1982**, *43*, 531.
(32) Birshtein, T. M.; Zhulina, E. B. *Polymer* **1984**, *25*, 1453.
(33) Douglas, J. F.; Freed, K. *Macromolecules* **1984**, *17*, 1854. See also: Miyake, A.; Freed, K. *Macromolecules* **1983**, *16*, 1228.
(34) Mazur, J.; McCrackin, F. *Macromolecules* **1977**, *10*, 326.
(35) Kolinski, A.; Sikorski, A. *J. Polym. Sci., Polym. Lett. Ed.* **1982**, *20*, 177.
(36) Kolinski, A.; Sikorski, A. *J. Polym. Sci., Polym. Chem. Ed.* **1982**, *20*, 3147.
(37) Sikorski, A.; Kolinski, A. *J. Polym. Sci., Polym. Chem. Ed.* **1984**, *22*, 97.
(38) Vlahos, C. H.; Kosmas, M. K. *Polymer* **1984**, *25*, 1607.
(39) Kohkhlov, A. R. *Polymer* **1978**, *19*, 1387.
(40) Khokhlov, A. R. *Polymer* **1981**, *22*, 447.
(41) Herman, D.; Kinning, D. J.; Thomas, E. L.; Fetters, L. J., in preparation.
(42) Aggarwal, S. L. *Polymer* **1976**, *17*, 938.

Studies of the Antenna Effect in Polymer Molecules. 8. Photophysics of Water-Soluble Copolymers of 1-Naphthylmethyl Methacrylate and Acrylic Acid

James E. Guillet* and W. Alan Rendall†

Department of Chemistry, University of Toronto, Toronto, Canada M5S 1A1.
Received November 9, 1984

ABSTRACT: Intramolecular singlet electronic energy transfer from naphthalene to anthracene end groups in copolymers of acrylic acid with 1-naphthylmethyl methacrylate has been studied. This work represents the first investigation of efficient singlet electronic energy transfer in such polymeric systems in the aqueous phase. Results in the aqueous phase are compared with those for the same polymers in dioxane. The efficiency of the energy-transfer process was greatly enhanced in aqueous media. In dioxane the energy-transfer efficiency was roughly 15%, while the same copolymers in the aqueous phase exhibited energy-transfer efficiencies up to 70%. Fluorescence decay measurements and time-resolved emission spectroscopy provide further details about the time scale of the energy-transfer process. In the aqueous phase the average energy-transfer time was substantially shorter than in dioxane. In addition, energy transfer to anthracene was observed to occur over a period of several tens of nanoseconds following excitation of the naphthalene chromophores.

Introduction

The existence of electronic energy transfer between chromophores attached to a polymer chain has been widely employed in accounting for certain aspects of polymer photophysics. For example, in the study of vinylaromatic polymers, Reid and Soutar[1,2] and Anderson et al.[3] have invoked singlet energy migration as an essential part of a model to describe excimer formation in terms of nearest-neighbor interactions in these systems. Other studies of excimer formation have also discussed the role of electronic energy transfer.[4-8]

The possibility of using polymer molecules bearing suitable donor and acceptor chromophores to produce synthetic antennae capable of efficiently modeling the light-harvesting function of the photosynthetic process has generated considerable interest in the study of energy migration and energy-transfer phenomena in polymer systems. Energy transfer to chemically bound traps in polymers was first described by Fox and Cozzens.[9] More recently Guillet and co-workers have shown that these processes can occur within a single polymer chain.[10-12]

Initially, intramolecular energy transfer was studied in poly(1-naphthyl methacrylate) (PNMA) polymers possessing terminal 9-vinylanthracene traps.[10,12] This work

†Current address: Department of Chemistry, University of Alberta, Edmonton, Canada T6G 2G2.

0024-9297/86/2219-0224$01.50/0